Acetylcholine-producing NK cells attenuate CNS inflammation via modulation of infiltrating monocytes/macrophages

Wei Jiang[a,b], Daojing Li[a], Ranran Han[a], Chao Zhang[a], Wei-Na Jin[a,b], Kristofer Wood[b], Qiang Liu[a,b], Fu-Dong Shi[a,b], and Junwei Hao[a,1]

[a]Department of Neurology, Tianjin Neurological Institute, Tianjin Medical University General Hospital, Tianjin 300052, China; and [b]Department of Neurology, Barrow Neurological Institute, St. Joseph's Hospital and Medical Center, Phoenix, AZ 85013

Edited by Lawrence Steinman, Stanford University School of Medicine, Stanford, CA, and approved June 13, 2017 (received for review April 3, 2017)

The nonneural cholinergic system of immune cells is pivotal for the maintenance of immunological homeostasis. Here we demonstrate the expression of choline acetyltransferase (ChAT) and cholinergic enzymes in murine natural killer (NK) cells. The capacity for acetylcholine synthesis by NK cells increased markedly under inflammatory conditions such as experimental autoimmune encephalomyelitis (EAE), in which ChAT expression escalated along with the maturation of NK cells. ChAT$^+$ and ChAT$^-$ NK cells displayed distinctive features in terms of cytotoxicity and chemokine/cytokine production. Transfer of ChAT$^+$ NK cells into the cerebral ventricles of CX3CR1$^{-/-}$ mice reduced brain and spinal cord damage after EAE induction, and decreased the numbers of CNS-infiltrating CCR2$^+$Ly6C^{hi} monocytes. ChAT$^+$ NK cells killed CCR2$^+$Ly6C^{hi} monocytes directly via the disruption of tolerance and inhibited the production of proinflammatory cytokines. Interestingly, ChAT$^+$ NK cells and CCR2$^+$Ly6C^{hi} monocytes formed immune synapses; moreover, the impact of ChAT$^+$ NK cells was mediated by α7-nicotinic acetylcholine receptors. Finally, the NK cell cholinergic system up-regulated in response to autoimmune activation in multiple sclerosis, perhaps reflecting the severity of disease. Therefore, this study extends our understanding of the nonneural cholinergic system and the protective immune effect of acetylcholine-producing NK cells in autoimmune diseases.

acetylcholine | NK cell | CCR2$^+$Ly6C^{hi} monocyte | immune homeostasis | EAE

Inflammation and immune responses within the central nervous system (CNS) are the causative features of multiple sclerosis (MS) (1), which afflicts ∼2.5 million individuals worldwide. MS and its animal model, experimental autoimmune encephalomyelitis (EAE), are characterized by immune cell infiltration of the CNS, demyelination, and axonal damage, thus leading to functional paralysis (2).

The cholinergic antiinflammatory system plays a well-established role in maintaining immune homeostasis in various inflammatory or autoimmune diseases (3, 4). The expression of choline acetyltransferase (ChAT) and synthesis of acetylcholine (ACh) have been proven in multiple immune cells, such as CD4$^+$ T cells, B cells, dendritic cells, and macrophages, by either inflammatory or neuronal stimulation; in turn, the presence of ChAT and ACh can outweigh the overactivated immune response (5, 6). During maturation, some immune cells gain the ability to synthesize ACh, which is an important participant in controlling the immune response through interaction with regional innate immune cells (6). However, whether NK cells express ChAT within organ-specific inflammatory environments during development and, if so, its role in immunity remain unclear.

The impact of NK cells on the outcome of CNS autoimmunity varies depending on the course of disease progression (7–10). The CD56^{bright} subset of human NK cells was shown to provide immune protection under MS conditions, the effect of which was proven and amplified by daclizumab or daclizumab high-yield process treatment (11–16). CNS-resident NK cells mediate immune suppression during the acute stage of CNS autoimmune diseases via cross-talk with microglia/macrophages of the CNS (17, 18). The reciprocal interaction between NK cells and monocytes/macrophages of the innate immune system has also been considered crucial for the immune activity of these cells in various inflammatory conditions (19–22). However, a more profound understanding of the detrimental and beneficial roles of macrophages in EAE has been reported, which relies on the new recognition of monocyte-derived macrophages being functionally distinct from microglia-derived macrophages (23–27). Among these cells, CCR2$^+$Ly6C^{hi} monocytes, which are rapidly recruited to the CNS and further transform into macrophages, proved to be crucial in EAE progression (24, 28, 29). The Ly6C^{hi} subset of monocytes was described as the most potent for NK cell activation (30). This background led us to reinvestigate the interaction between NK cells and the damage-evoking macrophages in EAE. Our previous work on EAE documented the immune protective effect of cholinergic antiinflammatory action, shown by inhibiting immune cell activation and inflammatory cytokine secretion (31–33). Additionally, we recently found that the migration of CCR2$^+$Ly6C^{hi} monocytes was largely inhibited by nicotine treatment, resulting from the effect of exogenous cholinergic antiinflammatory activity (34, 35). However, the existence of an

Significance

Acetylcholine (ACh) produced by neurons performs an array of functions that control cardiac, gastrointestinal, and other biosystems. Here we discovered that lymphocytic natural killer (NK) cells bear machinery that produces ACh. The activity of ACh-producing NK cells up-regulates during the disease flare of multiple sclerosis (MS) and may, therefore, reflect the pathologic state. In the mouse model of MS, experimental autoimmune encephalomyelitis, these ACh-producing NK cells can reduce the intensity of inflammation and autoimmune responses in the brain and spinal cord. Therefore, the nonneural cholinergic system, as reflected by ACh-producing NK cells, appeared to counteract aberrant immune responses and lessen brain damage. This observation offers insight into the therapeutic mechanisms of the Food and Drug Administration-approved drug daclizumab high-yield process for MS.

Author contributions: Q.L., F.-D.S., and J.H. designed research; W.J., D.L., R.H., and W.-N.J. performed research; W.J., C.Z., and K.W. analyzed data; and W.J., Q.L., F.-D.S., and J.H. wrote the paper.

The authors declare no conflict of interest.

This article is a PNAS Direct Submission.

Freely available online through the PNAS open access option.

Data deposition: The microarray data reported in this paper have been deposited in the Gene Expression Omnibus (GEO) database, www.ncbi.nlm.nih.gov/geo (accession no. GSE99126).

[1]To whom correspondence should be addressed. Email: hjw@tmu.edu.cn.

This article contains supporting information online at www.pnas.org/lookup/suppl/doi:10.1073/pnas.1705491114/-/DCSupplemental.

www.pnas.org/cgi/doi/10.1073/pnas.1705491114

endogenous cholinergic system in NK cells and its possible role in mediating the immune effect on infiltrating monocyte-derived macrophages are uncertain. Therefore, this study was performed to determine whether the cholinergic system exists in NK cells and, if so, how it contributes to an immune protective effect during inflammation.

Results

The Cholinergic System in NK Cells and Its Activation upon Immune Stimulation. NK cells from the spleens of mice were obtained by FACS sorting based on NK1.1 and CD3 expression. The purity of NK cells ($NK1.1^+CD3^-$) was above 95% after sorting (Fig. 1*A*). Total mRNA was extracted from the sorted NK cells, followed by reverse transcription. The expression of ChAT, vesicular ACh transporter (VAChT), acetylcholinesterase (AChE), and choline transporter 1 (CHT1) in murine NK cells was confirmed by amplified cDNA electrophoresis, with samples from brain cells used as a positive control (Fig. 1*B*). Western blot analyses were further conducted to identify the protein expression of ChAT, VAChT, AChE, and CHT1 in NK cells (Fig. 1*C*). To determine the capacity for ACh synthesis in NK cells, an established method for measuring concentrations was applied, with d_9-ACh used as the internal standard (36) (Fig. 1*D*). The detection limit of ACh concentration ranged from 0.05 to 5 ng/mL (Fig. 1*E*). When intracellular ACh production was quantified in NK cells by ultraperformance liquid-chromatography tandem mass spectrometry (UPLC-MS/MS), IL-2 and LPS stimulation of the cultured NK cells proved to increase their ACh production (0.06 ± 0.03 vs. 0.22 ± 0.07 ng/10^6 cells for control vs. IL-2 + LPS; $P < 0.05$) (Fig. 1*F*). Immune cells were isolated from the spleens of wild-type (WT) and ChAT-enhanced green fluorescent protein (eGFP) mice, and ChAT expression in total splenic immune cells as well as NK cells was measured based on eGFP level. Once again, we identified the presence of $ChAT^+$ immune cells in spleens from ChAT-eGFP mice compared with spleen cells from WT mice (6) (Fig. 1*G*). Interestingly, we found that a small portion of NK cells was $ChAT^+$ and that the expression increased upon IL-2 and LPS stimulation in vitro. IL-2 added alone had no obvious effect on ChAT expression in NK cells; however, LPS activation increased ChAT expression significantly in culture ($0.98 \pm 0.17\%$, $1.18 \pm 0.24\%$, and $2.98 \pm 0.45\%$ for control, IL-2 treatment, and IL-2 + LPS treatment, respectively; $P < 0.05$ when comparing control vs. IL-2 + LPS treatment or IL-2 vs. IL-2 + LPS treatment) (Fig. 1*H*). This ChAT-eGFP was expressed in NK cells constitutively, and LPS stimulation increased the expression markedly within 12 h of culture ($0.31 \pm 0.10\%$ vs. $0.98 \pm 0.17\%$, $0.22 \pm 0.07\%$ vs. $2.48 \pm 0.30\%$, $0.15 \pm 0.04\%$ vs. $2.98 \pm 0.45\%$, and $0.47 \pm 0.22\%$ vs. $2.73 \pm 0.32\%$, respectively, for WT vs. $ChAT\text{-}eGFP^+$ mice at 0, 12, 24, and 36 h; $P < 0.05$ for each time point) (Fig. 1*I*). These data confirm the existence of a cholinergic system in NK cells and its ability to up-regulate ACh synthesis during the acute phase of inflammatory stimulation.

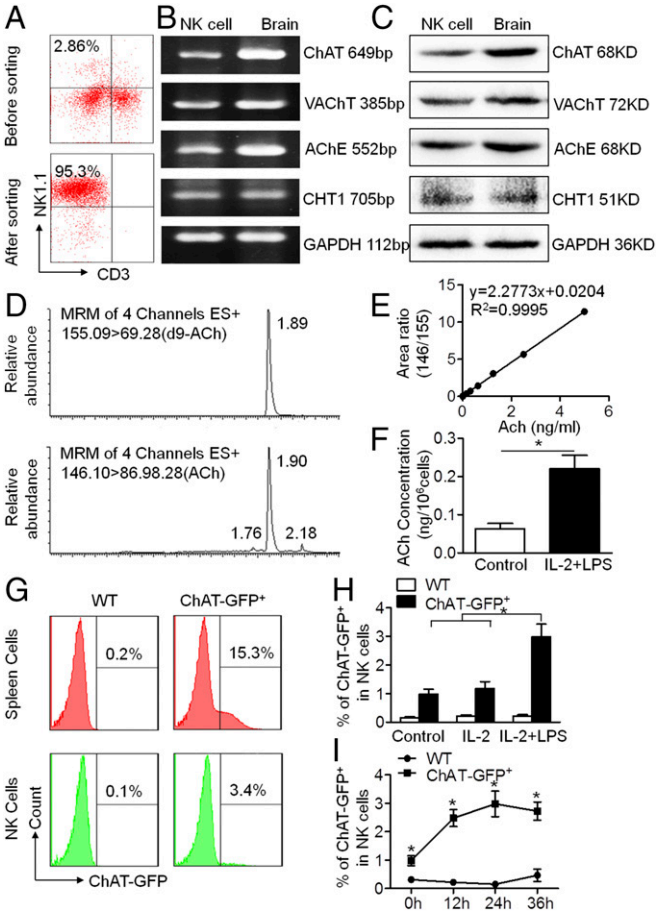

Fig. 1. Cholinergic system exists in murine NK cells, and acetylcholine synthesis increases under inflammatory stimulation. (*A*) NK cells ($NK1.1^+CD3^-$) from the spleens of C56BL/6 mice were sorted by FACS, producing a purity of above 95%. (*B* and *C*) Total mRNA and protein of sorted NK cells were extracted to identify key components of the cholinergic system by RT-PCR and Western blot, compared with the positive control from brain samples. Choline acetyltransferase, vesicular acetylcholine transporter, acetylcholinesterase, and choline transporter 1 were constitutively expressed and synthesized by murine NK cells. $n = 5$. (*D–F*) The concentration of intracellular ACh was determined by UPLC-MS/MS with d_9-ACh as the internal standard. Intracellular ACh production by NK cells increased under LPS stimulation with IL-2. $n = 6$ per group from two independent experiments. MRM, multiple reaction monitoring. (*G–I*) ChAT-eGFP expression in immune cells was counted by FACS. Percentages of $ChAT^+$ spleen immune cells gated by forward and side scatter or spleen NK cells ($NK1.1^+CD3^-$) were detected after culture. LPS enhanced $ChAT^+$ expression in NK cells above that in NK cells cultured with IL-2 alone or vehicle control. The percentage of $ChAT^+$ NK cells increased when cultured with IL-2 and LPS and peaked at 24 h following treatment. $n = 4$ to 6 per group from three independent experiments. Mean ± SEM. $^*P < 0.05$.

Induction of ChAT-eGFP During NK Cell Development and Phenotypic Maturation upon EAE Induction. To investigate the development of ChAT expression in NK cells and the underlying mechanisms of the cholinergic system's activation in response to inflammatory stimulation, we induced EAE in ChAT-eGFP mice and assessed ChAT-eGFP expression in splenic NK cell subsets. The development of NK cells can be divided into four stages based on CD11b expression in combination with CD27: $CD11b^-CD27^-$, $CD11b^-CD27^+$, $CD11b^+CD27^+$, and $CD11b^+CD27^-$ (Fig. 2*A*) (37, 38). ChAT-eGFP expression was evaluated in each of these NK cell subsets from the spleen in normal and EAE conditions. ChAT-eGFP expression increased during NK cell maturation in normal conditions. The percentage of $ChAT^+$ NK cells in the $CD11b^-CD27^-$ subset was the lowest, whereas ChAT-eGFP expression in $CD11b^+CD27^-$ was higher than in any other subset. EAE induction further enhanced ChAT-eGFP expression in the $CD11b^+CD27^+$ and $CD11b^+CD27^-$ subsets (Fig. 2 *B* and *C*).

The distribution of $ChAT^+$ NK cells changed dynamically with EAE progression. The progression of EAE over time is shown in Fig. 2*D*. NK cells originate in the bone marrow and then migrate into the peripheral blood and spleen, before finally infiltrating the CNS (8). The percentage of $ChAT^+$ NK cells in bone marrow cells (BMCs) did not change obviously during the course of EAE. However, the ChAT-eGFP expression of NK cells in the periphery reached a peak at 7 d post immunization (dpi), followed by a slight decrease at 12 dpi, and then fell back to normal levels at 16 dpi (Fig. 2*E*). Meanwhile, the percentage of $ChAT^+$ NK cells in the CNS reached the highest point at 16 dpi and fell at 20 dpi (Fig. 2*F*).

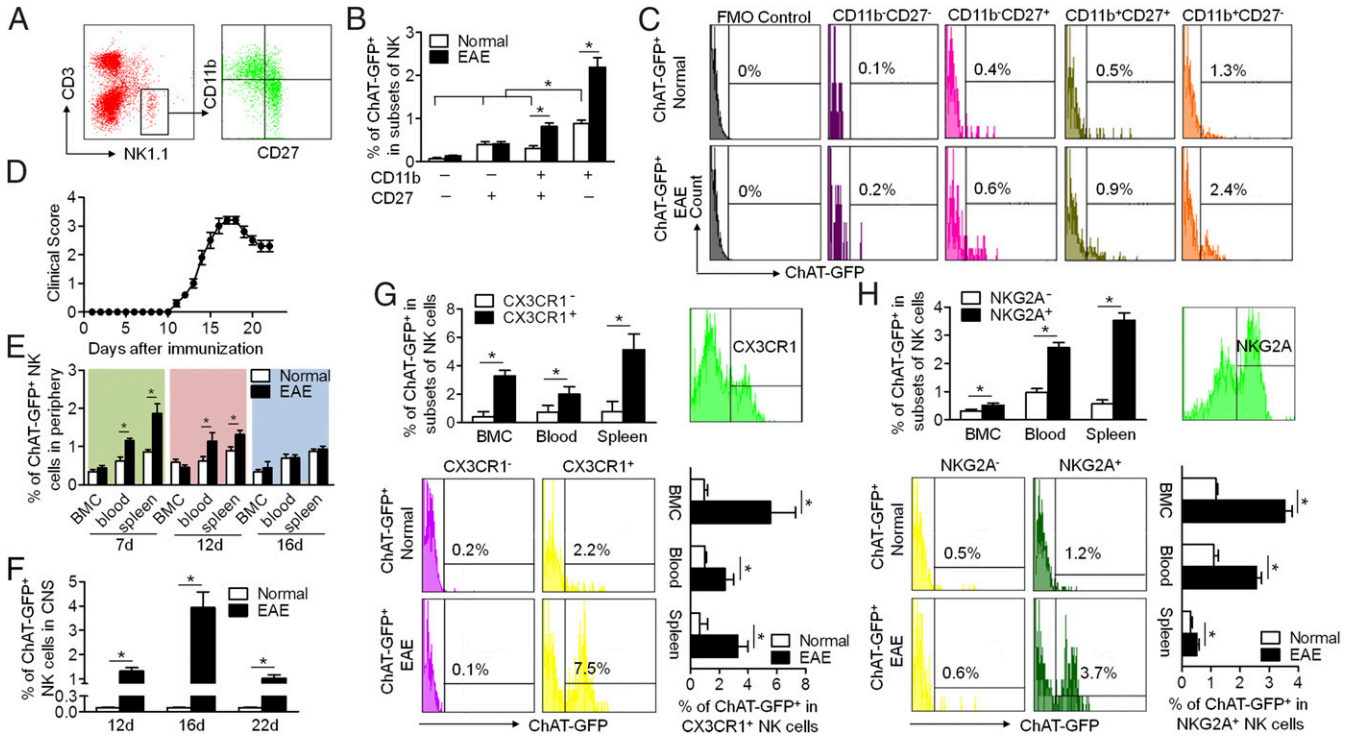

Fig. 2. ChAT-eGFP expression in murine NK cells during their development and phenotypic maturation upon EAE induction. (*A*) The development of NK cells is divisible into four stages based on the CD11b expression in combination with CD27. (*B* and *C*) ChAT-eGFP expression was determined on subsets of splenic NK cells at different development stages ($CD11b^{-}CD27^{-}$, $CD11b^{-}CD27^{+}$, $CD11b^{+}CD27^{+}$, $CD11b^{+}CD27^{-}$) in EAE mice. FMO control, fluorescence minus one control. ChAT expression increased during the maturation of NK cells under both normal and EAE conditions. In the presence of EAE, ChAT expression by mature NK cells increased dramatically. $n = 6$ per group. (*D*) The disease course of EAE was recorded: Initial manifestations occurred at 11 dpi; the peak was at around 16 dpi; and partial recovery was at 20 to 22 dpi. $n = 6$ per group. (*E*) During the course of EAE, the percentage of $ChAT^{+}$ NK cells in the periphery (blood and spleen) changed dynamically with disease progression, peaked at 7 dpi, recovered slightly at 12 dpi, and returned to normal at 16 dpi. During that time, ChAT-eGFP expression remained constant in naïve mice. $n = 6$ per group. (*F*) The percentage of $ChAT^{+}$ NK cells that infiltrated into the CNS reached a peak at 16 dpi and fell at 20 dpi in EAE mice. $n = 12$ per group. (*G*) Circulatory NK cells were divided phenotypically into subsets based on CX3CR1 expression. The expression of ChAT-eGFP in $CX3CR1^{+}$ NK cells exceeded that of $CX3CR1^{-}$ NK cells. The EAE status increased ChAT-eGFP expression in $CX3CR1^{+}$ NK cells. $n = 6$ per group. (*H*) Functional NK cells from the CNS were divided phenotypically into subsets based on NKG2A expression. The expression of ChAT-eGFP in $NKG2A^{+}$ NK cells surpassed that of $NKG2A^{-}$ NK cells. The EAE disease state increased ChAT-eGFP expression in $NKG2A^{+}$ NK cells. $n = 6$ per group from three independent experiments. Mean ± SEM. $^{*}P < 0.05$.

This result indicated that ChAT expression in NK cells is closely related to their migration during EAE progression.

The dynamic distribution of $ChAT^{+}$ NK cells in the periphery and CNS was associated with their migration during the disease course. NK cell homing to the CNS is largely dependent on the chemokine receptor CX3CR1 (18, 39, 40). Therefore, circulatory NK cells in the presence of EAE were phenotypically divided into two subsets based on CX3CR1 expression. Subsequent analysis revealed that ChAT-eGFP expression in $CX3CR1^{+}$ NK cells was higher than that of $CX3CR1^{-}$ NK cells from bone marrow, blood, and spleen. Additionally, the ChAT-eGFP expression in $CX3CR1^{+}$ NK cells increased upon EAE induction (Fig. 2*G*). The phenotype of a CNS-infiltrated NK cell determines its role in the immune activity of EAE (11, 17). Functional NK cells from the CNS of EAE animals were divided based on NKG2A expression. The percentage of $ChAT\text{-}eGFP^{+}$ expression in $NKG2A^{+}$ NK cells was higher than that of $NKG2A^{-}$ NK cells. The ChAT-eGFP expression in $NKG2A^{+}$ NK cells then increased upon EAE induction (Fig. 2*H*). Overall, these data indicate that ChAT expression is induced during NK cell maturation and is associated with NK cell subtypes that possess specific mobility and function in the EAE environment.

ChAT Expression Is Associated with a Distinct Gene-Expression Profile of NK Cells. To gain more evidence of the potential functional difference between $ChAT^{+}$ NK cells and $ChAT^{-}$ NK cells, an mRNA microarray procedure was conducted. This method enabled analysis of these cells' gene-expression patterns. Interestingly, a clear delineation between $ChAT^{+}$ NK cells and $ChAT^{-}$ NK cells was observed, with a total of 300 genes overexpressed and 941 genes underexpressed in $ChAT^{+}$ NK cells (Fig. 3*A*). The difference in expression was defined as more than a twofold change ($P < 0.05$) (Fig. 3*B*), demonstrating that $ChAT^{+}$ NK cells and $ChAT^{-}$ NK cells have distinctly different gene profiles. To better understand the meaning of this outcome, we analyzed gene ontology (GO) in terms of clusters of up-regulated or down-regulated genes using the DAVID (Database for Annotation, Visualization and Integrated Discovery; https://david.ncifcrf.gov/) functional annotation tool. The differentially expressed genes belonged to several functional families, including those of NK cell cytotoxicity, chemokines, cytokines, and other components of immune responses. $ChAT^{+}$ NK cells mainly overexpressed genes related to cytokines and chemokines, which are critically involved in mediating immune responses and chemotaxis under inflammatory conditions ($P < 0.05$). However, the down-regulated genes in $ChAT^{+}$ NK cells were most relevant to the cytotoxicity of NK cells according to GO and Kyoto Encyclopedia of Genes and Genomes analysis ($P < 0.05$), which indicated the potential immune regulatory role of this subset (Fig. 3*C*). Overall, $ChAT^{+}$ NK cells appeared to display a more activated phenotype toward immune regulation than the $ChAT^{-}$ counterparts in preserving homeostasis.

$ChAT^{+}$ NK Cells Reduce Pathologic Damage and Improve Neural Functions of EAE Mice. Because $ChAT^{+}$ NK cells clearly differed from $ChAT^{-}$ NK cells based on gene expression, further work was conducted to shed light on the functions of those cells in

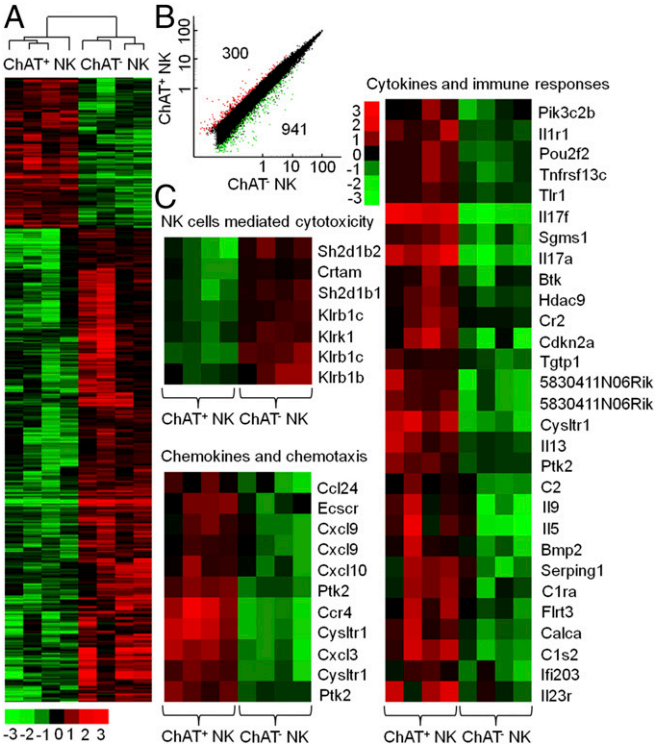

Fig. 3. mRNA microarray analysis reveals a distinctive expression profile of ChAT$^+$ NK cells. ChAT$^+$ NK cells and ChAT$^-$ NK cells were sorted by flow cytometry based on eGFP expression to identify their genetic differences. (*A*) A total of 300 genes was overexpressed and 941 genes underexpressed in ChAT$^+$ NK cells compared with ChAT$^-$ NK cells, with a clear delineation. (*B*) The two groups differed in expression by more than twofold, with a corrected P value < 0.05. (*C*) According to gene ontology analysis with the DAVID functional annotation tool, genes expressed in ChAT$^+$ NK cells represented an up-regulation in immune responses and chemotaxis but a decrease in cytotoxicity. $n = 4$ per group.

EAE. In CX3CR1$^{-/-}$ mice with EAE, NK cells failed to be recruited into the CNS, thus exacerbating disease severity (39). CX3CR1$^{-/-}$ mice without CNS-infiltrating NK cells exhibited similar EAE severity to WT mice subjected to systemic NK cell depletion, indicating the crucial immune protective role of CNS-infiltrating NK cells rather than NK cells in the periphery (32). Thus, in our experiments, ChAT$^-$ NK cells and ChAT$^+$ NK cells (both from mature CD11b$^+$CD27$^-$ NK cell populations) were transplanted into the cerebroventricles of CX3CR1$^{-/-}$ mice, which showed relieved disease severity, although ChAT$^+$ NK cell implantation showed enhanced immune protective effects compared with ChAT$^-$ NK cells (Fig. 4). CX3CR1$^{-/-}$ mice showed earlier disease onset and higher scores for clinical symptoms of EAE from 12 dpi and lasting until 22 dpi. However, ChAT$^+$ NK cell implantation delayed disease onset and reduced clinical scores in CX3CR1$^{-/-}$ mice more significantly than ChAT$^-$ NK cells (Fig. 4 *A*–*C*). When 7-T MRI scans were conducted to detect demyelinated lesions in the brains and spinal cords of EAE mice, increased signal intensity was present in the periventricular region of the brain and lumbar enlargement of the spinal cord. The cumulative lesion volumes showed less demyelination in the ChAT$^+$ NK cell-implanted groups ($3.05 \pm 0.32/mm^3$, $2.15 \pm 0.12/mm^3$, and $1.14 \pm 0.13/mm^3$ for vehicle, ChAT$^-$ NK cell, and ChAT$^+$ NK cell implantation, respectively; $P < 0.05$) (Fig. 4 *D* and *E*). Hematoxylin & eosin (H&E) staining and Luxol fast blue (LFB) staining were then performed on spinal cord samples to visualize cell infiltration and demyelination. Cumulative results showed less accumulation of infiltrating cells (47.14 ± 2.86%, 36.86 ± 1.96%, and 28.56 ± 1.37% for vehicle, ChAT$^-$ NK cell, and ChAT$^+$ NK cell implantation; $P < 0.05$) and demyelination after ChAT$^+$ NK cell implantation (28.86 ± 2.20%, 20.29 ± 1.73%, and 11.43 ± 1.51% for vehicle, ChAT$^-$ NK cell, and ChAT$^+$ NK cell implantation; $P < 0.05$). After immunofluorescent staining with myelin basic protein (MBP), we witnessed aggravated demyelination along with a greater accumulation of cells, as indicated by DAPI staining in this lesion. However, ChAT$^+$ NK cell implantation relieved this damage from demyelination (37.29 ± 3.40%, 27.63 ± 3.29%, and 14.36 ± 1.56% for vehicle, ChAT$^-$ NK cell, and ChAT$^+$ NK cell implantation; $P < 0.05$) (Fig. 4 *F*–*I*). Therefore, this outcome indicates that ACh-producing NK cells act as an important subset of NK cells in modulating immunity in CNS autoimmune disease.

ChAT$^+$ NK Cells Diminish Accumulated CCR2$^+$Ly6C^{hi} Monocytes and Modify the Cytokine Microenvironment in the CNS. CNS demyelination is initiated by immune cell infiltration and subsequent inflammatory responses of innate and adaptive immunity within the CNS (41). To understand the potential interactions of ChAT$^+$ NK cells with CNS resident or infiltrative cells in mediating immune protection, we conducted further analysis. After ChAT$^+$ NK cell implantation into the CNS of EAE mice, the content of infiltrating neutrophils (CD11b$^+$Ly6G$^+$), CD8$^+$ T cells (CD3$^+$CD8$^+$), B cells (CD3$^-$CD19$^+$), and resident microglia (CD11b$^+$CD45^{low}) did not change significantly (Fig. 5 *A* and *B*); however, the total number of CD4$^+$ T cells (CD3$^+$CD4$^+$) tended to decrease (14.97 ± 1.4% vs. 10.72 ± 1.73%; $P = 0.083$). Additionally, fewer total numbers of monocytes (CD11b$^+$CD45^{hi}) were present within the CNS of mice that received ChAT$^+$ NK cell implantation than ChAT$^-$ NK cell implantation (7.82 ± 1.33% vs. 12.07 ± 1.15%; $P < 0.05$) (Fig. 5 *A* and *B*). CCR2$^+$Ly6C^{hi} monocytes (CD11b$^+$Ly6G$^-$CCR2$^+$Ly6C^{hi}) are known to play an important role in the pathogenesis of EAE soon after infiltrating into the CNS (24, 28, 29). In our hands, flow cytometry showed large numbers of CCR2$^+$Ly6C^{hi} monocytes in the CNS of the CX3CR1$^{-/-}$ group but far fewer in the ChAT$^+$ NK cell-implanted groups (20.00 ± 3.38%, 11.45 ± 0.84%, and 5.97 ± 1.33% for vehicle, ChAT$^-$ NK cell, and ChAT$^+$ NK cell implantation; $P < 0.05$), without altering their distribution in the spleen (29.50 ± 2.78%, 30.75 ± 2.66%, and 32.25 ± 2.06% for vehicle, ChAT$^-$ NK cell, and ChAT$^+$ NK cell implantation; $P > 0.05$) (Fig. 5 *C* and *D*). The gating strategy for these immune cells was conducted as done previously (34).

Furthermore, we found that the loss of MBP in the spinal cords of EAE mice coincided with the large accumulation of CCR2$^+$-infiltrating monocytes/macrophages, rather than the number of resident microglia that were GFP$^+$ with distinct morphology in CX3CR1$^{GFP/GFP}$(CX3CR1$^{-/-}$) mice ($62.5 \pm 11.04/mm^2$ vs. $1518 \pm 70.19/mm^2$; $P < 0.05$) (Fig. 5 *E*, *F*, and *I*). A better scenario ensued for ChAT$^-$ NK cell-implanted mice, which underwent less severe demyelination with fewer CCR2$^+$-infiltrating monocytes ($1518 \pm 70.19/mm^2$ vs. $1215.33 \pm 67.56/mm^2$; $P < 0.05$) (Fig. 5 *G* and *I*). Interestingly, ChAT$^+$ NK cell implantation into CX3CR1$^{GFP/GFP}$ mice seemed to be efficacious in reducing the numbers of CCR2$^+$-infiltrated monocytes/macrophages ($1215.33 \pm 67.56/mm^2$ vs. $664.5 \pm 55.69/mm^2$; $P < 0.05$) rather than the resident microglia, with the result that demyelination decreased (Fig. 5 *H* and *I*).

The altered immune cell distribution within the CNS could be substantially affected by the cytokine microenvironment. RT-PCR conducted on the brain samples showed decreased expression of TNF-α, IL-1β, IL-6, and IL-12 relative to the internal standard of hypoxanthine phosphoribosyltransferase 1 (HPRT-1) expression. Meanwhile, the change in IL-10 expression was negligible (Fig. 5*J*). These data indicate that the immune protective effect of ChAT$^+$ NK cells in EAE was exerted by shaping the distribution of CCR2$^+$ Ly6C^{hi} monocytes and the cytokine microenvironment in the CNS.

Reciprocal Chemoattraction Between ChAT$^+$ NK Cells and CCR2$^+$ Ly6C^{hi} Monocytes. To explore the underlying mechanisms that enable ChAT$^+$ NK cells to reduce CCR2$^+$Ly6C^{hi} monocyte content within the CNS, the communication between these cells was investigated. Immunofluorescent staining of the CD11b$^+$CCR2$^+$

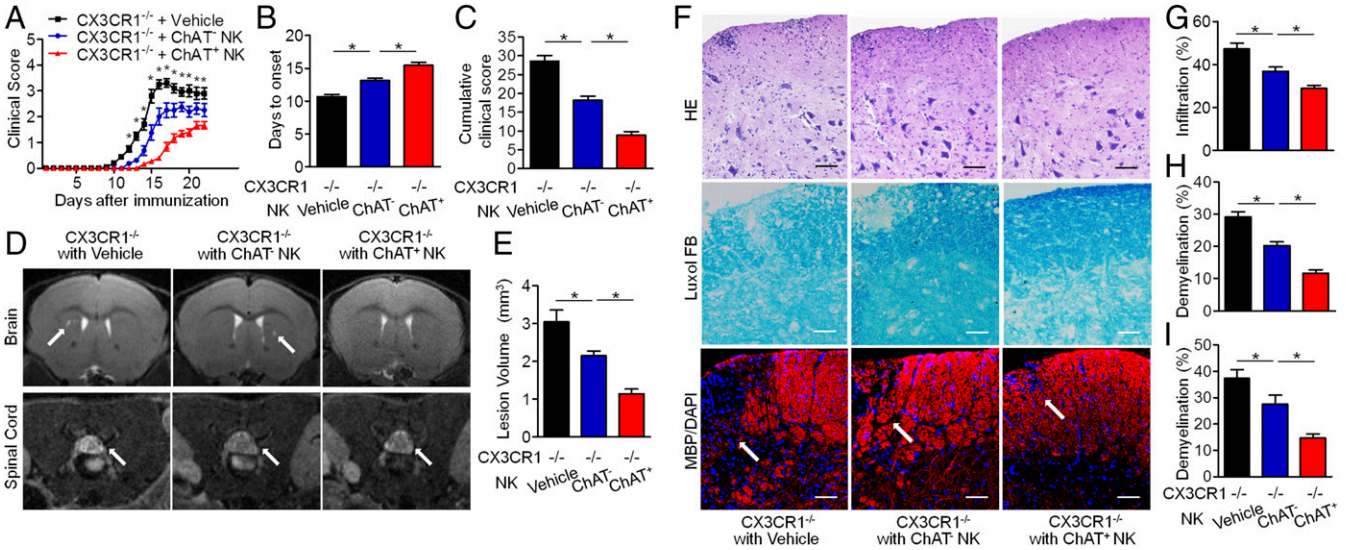

Fig. 4. ChAT$^+$ NK cells have immune protective effects in the CNS of EAE mice. (*A*) Vehicle, ChAT$^-$, or ChAT$^+$ NK cells were implanted into cerebral ventricles of CX3CR1$^{-/-}$ mice 10 d after EAE induction. The clinical scores of CX3CR1$^{-/-}$ mice without treatment exceeded those implanted with NK cells from 12 to 22 dpi. ChAT$^+$ NK cell implantation alleviated disease progression, as evident from lower clinical scores during the 12 to 22 dpi period. (*B*) The day of disease onset was earlier in CX3CR1$^{-/-}$ mice and was significantly delayed by ChAT$^+$ NK cell implantation. (*C*) The cumulative clinical score of CX3CR1$^{-/-}$ mice was higher than that of CX3CR1$^{-/-}$ mice with ChAT$^-$ NK cells, and was significantly reduced by ChAT$^+$ NK cell implantation. $n = 15$ per group for *A*–*C*. (*D* and *E*) T2-weighted images of brain and spinal cord samples from EAE mice were obtained by 7-T MRI. Arrows indicate lesions of increased signal intensity in the brain and spinal cord, which was reduced by ChAT$^+$ NK treatment. (*F*–*I*) H&E staining shows immune cell infiltration into the spinal cord. LFB and MBP staining depict demyelination of the CNS along with large accumulations of immune cells in the lesion. Arrows indicate the demyelinated lesions by MBP staining. The statistics of demyelination reflected by Luxol FB (H) and MBP/DAPI (I) staining are shown. The implantation of ChAT$^+$ NK cells reduced demyelination as well as decreasing the regional concentration of immune cells. $n =$ 10 per group for *D*–*I*. Data are representative of six independent experiments. Mean ± SEM. *$P < 0.05$. (Scale bars, 100 μm.)

monocytes and ChAT$^+$ NK cells within the CNS showed the spatial proximity of these cells in EAE mice, which provided a favorable environment for the interaction between CCR2$^+$Ly6C^{hi} monocytes and ChAT$^+$ NK cells (Fig. 6*A*). To further ensure this occurrence, the chemoattractive effects of these cells were confirmed by transwell experiments. ChAT$^+$ or ChAT$^-$ NK cells were loaded into the upper chamber of the transwell system, and bone marrow-derived macrophages that were purified to yield a CCR2$^+$Ly6C^{hi} population were loaded into the lower chamber. After 5 h of coculture, cells in the lower chamber were collected, and migrated NK cells were identified by FACS staining. The migratory ability of ChAT$^+$ NK cells was much greater than that of ChAT$^-$ NK cells (Fig. 6*C*). To investigate whether ChAT expression increased during migration or after encountering CCR2$^+$Ly6C^{hi} monocytes, the ChAT expression of migrated NK cells was evaluated. Only a limited number of migrated NK cells originating from the ChAT$^-$ upper chambers were found to become ChAT$^+$ (Fig. 6*B*). The probable cause was the cytokine microenvironment or intercellular action with CCR2$^+$Ly6C^{hi} monocytes, thereby facilitating NK cell expression of ChAT. In the transwell system, amounts of the cytokines IFN-γ, TNF-α, and GM-CSF expressed by migrated ChAT$^+$ NK cells from the lower chamber were higher than that of the ChAT$^-$ NK cells from the upper chamber according to RT-PCR detection, as was also seen for the expression of CCL3 and CCL4 (Fig. 6 *B* and *D*). Meanwhile, mRNA expression profiling indicated that, compared with the other monocyte populations, CCR2$^+$Ly6C^{hi} monocytes produced more of the chemokines CCL3, CCL4, CCL5, CXCL10, and CXCL11 as well as the cytokines IL-12, IL-15, and IL-18 (Fig. 6 *E* and *F*). These results better elucidate the chemoattraction between ChAT$^+$ NK cells and CCR2$^+$Ly6C^{hi} monocytes, which communicate through the production of multiple cytokines and chemokines.

Immune Synapses Between ChAT$^+$ NK Cells and CCR2$^+$Ly6C^{hi} Monocytes Involve the NKG2A–Qa-1 Pathway and α7-Nicotinic Acetylcholine Receptors. Based on the colocalization of CCR2$^+$ infiltrative monocytes and ChAT$^+$ NK cells in the CNS and the reciprocal chemoattraction and communication between CCR2$^+$Ly6C^{hi} monocytes and ChAT$^+$ NK cells, we wondered whether the decrease of CCR2$^+$Ly6C^{hi} monocytes in the CNS implanted with ChAT$^+$ NK cells was executed via immune synapses formed between these cells and triggering the lytic activity or passing of an immune suppressive message. First, conjugate formation was quantified by FACS analysis, which indicated more synapse formation between ChAT$^+$ NK cells and CCR2$^+$Ly6C^{hi} monocytes than with ChAT$^-$ NK cells (Fig. S1 *A*–*C*). Immunological imaging analysis of the immune synapse showed the redistribution of α7-nicotinic acetylcholine receptors (α7nAChRs) on the surfaces of CCR2$^+$Ly6C^{hi} monocytes accumulated toward the synapse with ChAT$^+$ NK cells rather than evenly distributed on the surfaces of CCR2$^+$Ly6C^{hi} monocytes alone (Fig. 7*A*). However, no polarization of α7nAChRs in CCR2$^+$Ly6C^{hi} monocytes was observed toward ChAT$^-$ NK cells (Fig. S1 *D* and *F*), thus indicating the potential involvement of these receptors in the communication within synapses. The decreased expression of TNF-α, IL-1β, and IL-12 cytokines in CCR2$^+$Ly6C^{hi} monocytes after coculture with ChAT$^+$ NK cells (1.97 ± 0.18 vs. 1.17 ± 0.24, 0.84 ± 0.04 vs. 0.43 ± 0.12, and 1.25 ± 0.14 vs. 0.62 ± 0.16 relative expression for TNF-α, IL-1β, and IL-12 after coculture with ChAT$^-$ NK vs. ChAT$^+$ NK cells, respectively; $P < 0.05$) was reversed in α7nAChR knockout (KO) CCR2$^+$Ly6C^{hi} monocytes (1.83 ± 0.13 vs. 1.99 ± 0.35, 0.90 ± 0.19 vs. 0.80 ± 0.09, and 1.40 ± 0.27 vs. 1.28 ± 0.35 relative expression for TNF-α, IL-1β, and IL-12, respectively, after coculture with ChAT$^-$ NK vs. ChAT$^+$ NK cells; $P > 0.05$). This series of interactions indicates the important role of α7nAChR in mediating this activity. After culturing with ChAT$^+$ NK cells, the expression of IL-10 in CCR2$^+$Ly6C^{hi} monocytes from WT (0.52 ± 0.09 vs. 0.52 ± 0.07 relative expression; $P > 0.05$) or α7nAChR KO mice (0.52 ± 0.09 vs. 0.51 ± 0.17 relative expression; $P > 0.05$) did not change (Fig. 7*C*).

Perforin staining within the synapse also revealed the existence of cytotoxic activity during the intercellular action (Fig. 7*B* and Fig. S1 *E* and *G*). To understand the mechanism that instigated

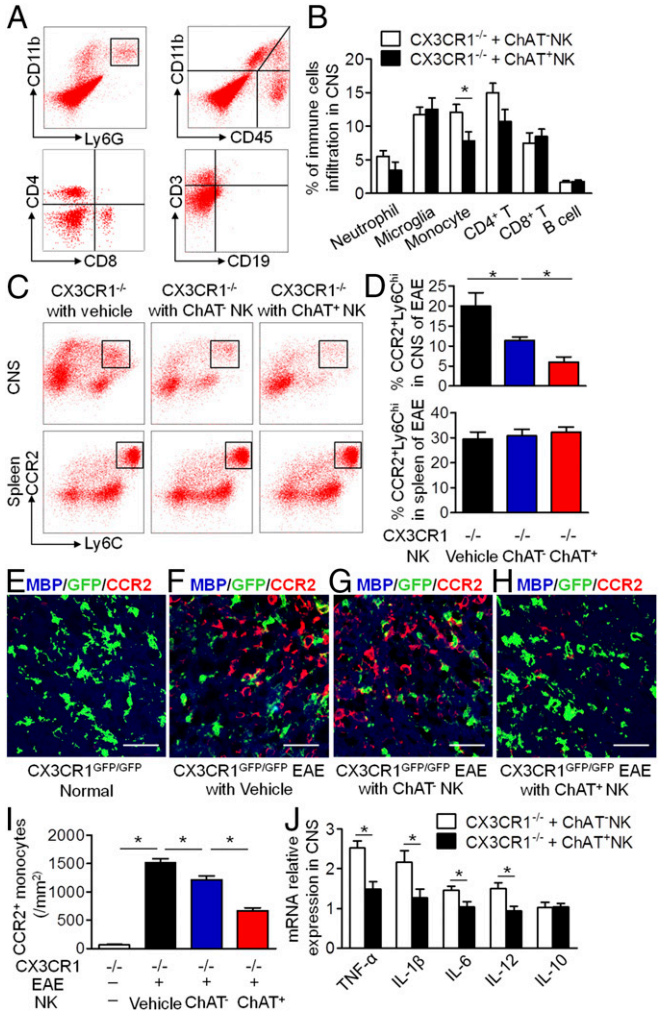

Fig. 5. ChAT$^+$ NK cells influence the distribution of CCR2$^+$Ly6C^{hi} monocytes and the cytokine microenvironment in the CNS of EAE mice. (*A* and *B*) The percentages of CNS-infiltrated neutrophils (CD11b$^+$Ly6G$^+$), CD8$^+$ T cells, B cells (CD3$^-$CD19$^+$), and microglia (CD11b$^+$CD45^{low}) were not changed by ChAT$^+$ NK cell implantation. However, the numbers of infiltrated monocytes and CD4$^+$ T cells ($P = 0.083$) decreased in ChAT$^+$ NK cell-implanted groups. $n = 6$ per group. (*C* and *D*) The percentage of CCR2$^+$Ly6C^{hi} monocytes in the CNS and spleen of CX3CR1$^{-/-}$, CX3CR1$^{-/-}$ with ChAT$^-$ NK cells, and CX3CR1$^{-/-}$ mice with ChAT$^+$ NK cells. ChAT$^+$ NK cell implantation significantly decreased the numbers of CCR2$^+$Ly6C^{hi} monocytes in the CNS without altering their distribution in the spleen. $n = 6$ per group. (*E–I*) MBP staining with CCR2 revealed a decrease of infiltrated CCR2$^+$ monocytes/macrophages and reduced demyelination from ChAT$^+$ NK cell treatment, without much effect on resident microglia (CX3CR1-GFP$^+$). $n = 9$ per group. (*J*) Relative mRNA expression of TNF-α, IL-1β, IL-6, IL-12, and IL-10 to HPRT-1 as the internal standard in CNS. $n = 6$ per group. Data are representative of three independent experiments. Mean ± SEM. $^*P < 0.05$. (Scale bars, 40 μm.)

the killing of autologous target cells by ChAT$^+$ NK cells and mediated the antiinflammatory effect, further experiments were conducted. Coculturing CCR2$^+$Ly6C^{hi} monocytes with ChAT$^+$ NK cells resulted in their significantly reduced expression of Qa-1 compared with those cocultured with ChAT$^-$ NK cells (20.97 ± 1.65% vs. 15.53 ± 1.59%; $P < 0.05$) (Fig. 7 *D* and *E*). Meanwhile, similarly sorted NK cells were cocultured with CCR2$^+$Ly6C^{hi} monocytes, after which the expression of ChAT-eGFP (0.93 ± 0.19% vs. 2.33 ± 0.27%; $P < 0.05$) and NKG2A (15.43 ± 1.33% vs. 22.03 ± 2.35%; $P < 0.05$) increased significantly. However, the expression of NKG2D in NK cells was not significantly different after the coculture (0.30 ± 0.12% vs. 0.47 ± 0.18%; $P > 0.05$) (Fig. 7 *F* and *G*). The viability of CCR2$^+$Ly6C^{hi} monocytes in the coculture system was then evaluated by 7-AAD staining (Fig. 7*H*). The susceptibility to killing by ChAT$^+$ NK cells was reduced by Qa-1 up-regulation through lentivirus transfection, at effector: target ratios of 25:1, 10:1, and 5:1 (28.20 ± 1.39% vs. 19.80 ± 1.59%, 18.60 ± 1.30% vs. 14.37 ± 1.18%, and 15.83 ± 0.12% vs. 12.33 ± 1.02% for 25:1, 10:1, and 5:1, respectively; $P < 0.05$). However, Qa-1 down-regulation exacerbated the likelihood of being killed by ChAT$^+$ NK cells (28.20 ± 1.39% vs. 33.57 ± 1.73%, 18.60 ± 1.30% vs. 26.10 ± 1.44%, and 15.83 ± 0.12% vs. 21.70 ± 2.12% for 25:1, 10:1, and 5:1, respectively; $P < 0.05$) (Fig. 7*I*).

For adoptive transfers to induce EAE, myelin oligodendrocyte glycoprotein (MOG)-responsive T cells and CCR2$^+$Ly6C^{hi} monocytes were injected into Rag2$^{-/-}$ γc$^{-/-}$ mice. ChAT$^+$ NK cell implantation alleviated disease severity during EAE progression but had no effect on mice transferred with MOG-responsive T cells and α7nAChR KO CCR2$^+$Ly6C^{hi} monocytes (Fig. 7*J*). The foregoing results indicate that α7nAChRs and the Qa-1–NKG2A pathway in the immune synapse between ChAT$^+$ NK cells and CCR2$^+$Ly6C^{hi} monocytes are important participants in the immune regulatory effect of ChAT$^+$ NK cells toward CCR2$^+$Ly6C^{hi} monocytes, through direct killing as well as modification of cytokine secretion.

Up-Regulation of Cholinergic Activity in NK Cells from MS Patients. To determine the translational value of the foregoing observation to humans, the cholinergic system of NK cells from human peripheral blood was identified with determination of intracellular ACh production. NK cells were sorted from human peripheral blood samples by FACS to be used as a source of mRNA and protein extraction. RT-PCR and Western blot analysis of these human NK cells confirmed the expression of ChAT, VAChT, AChE, and CHT1, which are essential components of the cholinergic system (Fig. 8 *A* and *B*). Immunofluorescent staining of brain samples from MS patients also showed ChAT expression in infiltrated NK cells (NKp46$^+$ChAT$^+$GFAP$^-$) (Fig. 8*C*). Staining of GFAP was involved to exclude astrocytes, which were reported to express NKp46 under an activated status in lesions of MS patients as well (42). Pathologic staining with MBP then revealed that those ChAT$^+$ NK cells were preferentially located in the active demyelinated lesions of MS patients (Fig. 8*C*). Further, ACh production by NK cells from the peripheral blood was confirmed by UPLC-MS/MS detection. The intracellular concentration of ACh in NK cells from MS patients was higher than that from healthy individuals (0.1841 ± 0.00441 vs. 0.0187 ± 0.00561 ng/10^6 cells; $P < 0.05$) (Fig. 8*D*). Additionally, the intracellular ACh concentrations showed a positive correlation with EDSS (Expanded Disability Status Scale) scores of the MS patients ($P < 0.05$) (Fig. 8*E*). The T2 high-intensity lesions detected in MRI scans from MS patients also revealed a positive correlation between ACh concentration and lesion volume ($P < 0.05$) or the multiplicity of the lesions ($P < 0.05$) (Fig. 8 *F–H*). Overall, these data indicated that nonneural cholinergic activity of NK cells is up-regulated in CNS autoimmune disease and may be attributed to compensatory up-regulation in response to an overactivated autoimmune reaction in the MS setting. Therefore, the determination of ACh level in NK cells from the periphery could be an option for predicting the prognosis of patients with MS.

Discussion

Our results depict the antiinflammatory effect of ChAT$^+$ NK cells in CNS inflammation involving the NKG2A–Qa-1 pathway and α7-nAChRs. Considering the widespread distribution of α7nAChRs, ChAT$^+$ immune cells could modulate the immune balance through the receptors especially under conditions of inflammatory disease (5, 6, 43). The expression and up-regulation of the nonneural cholinergic system are fine-tuned via chemical or neural stimulation as a mechanism to regulate or counteract the immune system (44,

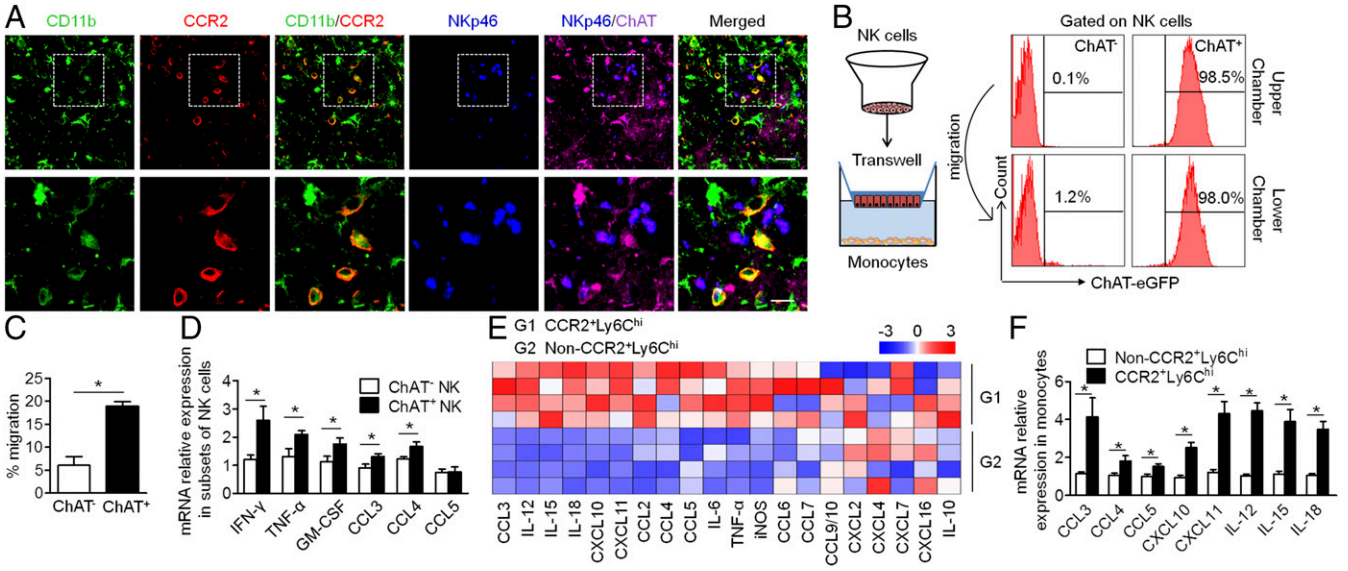

Fig. 6. ChAT$^+$ NK cells and CCR2$^+$Ly6C^{hi} monocytes are attracted reciprocally and communicate through various cytokines and chemokines. (*A*) ChAT$^+$ NK cells and CD11b$^+$CCR2$^+$ infiltrative monocytes are colocalized in the CNS of EAE mice under confocal observation. Images are representative of three independent experiments. [Scale bars, 40 μm (*Upper*) and 20 μm (*Lower*).] (*B* and *C*) Sorted ChAT$^+$ or ChAT$^-$ NK cells were loaded into the upper chamber of the transwell system, and the lower chamber was loaded with bone marrow-derived monocytes. After 5 h of migration, the number of migrated NK cells was determined by FACS and is shown as a percentage of the total amount loaded. ChAT expression in the lower chamber that migrated from the ChAT$^+$ or ChAT$^-$ upper chamber was also evaluated. $n = 6$ per group from three independent experiments. (*D*) The relative mRNA expression of IFN-γ, TNF-α, GM-CSF, CCL3, CCL4, and CCL5 was detected in ChAT$^+$ NK cells and ChAT$^-$ NK cells. $n = 6$ per group of three independent experiments. (*E*) The mRNA expression of various cytokines/chemokines in CCR2$^+$Ly6C^{hi} monocytes and non-CCR2$^+$Ly6C^{hi} monocytes was detected. The expression level relative to the internal standard HPRT-1 appears in the heat map after *Z* transformation. (*F*) Among the genes detected, CCL3, CCL4, CCL5, CXCL10, CXCL11, IL-12, IL-15, and IL-18 were the most highly produced by CCR2$^+$Ly6C^{hi} monocytes. $n = 6$ per group of three independent experiments. Mean ± SEM. $^*P < 0.05$.

45). Different from T or B cells, NK cells presumably respond quickly as part of innate immunity during inflammation. Therefore, an up-regulated expression of the cholinergic system in NK cells during the acute phase of inflammation could have a significant impact to restrict CNS inflammation.

NK cells develop functionally as they circulate through various organs after migrating from the bone marrow (46–49). Here, ChAT-eGFP expression was observed mostly in NK cell subsets of a mature phenotype in the periphery and was enhanced after EAE induction, which may correspond to the finding that more NK cells are mobilized under inflammatory conditions, possibly facilitating their maturation or activation (15, 50). However, the percentage of NK cells with ChAT expression did not seem to show a simple positive relationship with the severity of disease in certain organs. However, the acquisition and dynamic distribution of ChAT$^+$ NK cells in the periphery and CNS along with disease progression reflected the close association between NK cell migration and ChAT expression. ChAT$^+$ NK cells appear to possess greater migratory ability and are more readily recruited to sites of CNS injury. The more significant effect of ChAT$^+$ vs. ChAT$^-$ NK cells via the i.v. transfer to restrict CNS inflammation also supports this postulation (Fig. S2). Additionally, genome analysis depicted a distinctive expression profile of ChAT$^+$ NK cells in terms of greater cytokine and chemokine production than their ChAT$^-$ counterparts. Therefore, expression of the cholinergic system in NK cells is related to their propensity for CNS homing as well as phenotypic activation with regulatory functions.

Unlike the experiments with transgenic mice that selectively lack T or B cells for functional study in vivo, no mice are available that selectively lack NK cells (51–53). Consequently, we elected to use CX3CR1$^{-/-}$ mice, because the loss of CX3CR1 on NK cells impairs the capability of NK cells to home in to the CNS. Functional analysis of ChAT$^+$ NK cells after their transplantation into CX3CR1$^{-/-}$ mice revealed a dramatic influence on the distribution of CCR2$^+$Ly6C^{hi} monocytes within the CNS, without much effect on microglia, CD8$^+$ T cells, B cells, or neutrophils. The initiation and progression of EAE are associated with infiltration of immune cells into the CNS and subsequent immune responses between the adaptive and innate immune systems (54). CCR2$^+$Ly6C^{hi} monocytes are among the earliest monocytes to infiltrate the CNS and are crucial for the development of EAE (55–58). Therefore, the decrease of CCR2$^+$Ly6C^{hi} monocytes within the CNS after ChAT$^+$ NK cell implantation appeared to contribute greatly to the lessening of EAE symptoms.

Unlike previous findings (18), the effect of these transplanted ChAT$^+$ NK cells in the CNS was a preferential reduction of infiltrated monocytes/macrophages rather than resident microglia. The cause may have been chemotaxis between these cells and the timing of transplant intervention, during which the numbers of infiltrating monocytes exceeded that of the resident microglia. Even though the overall distribution of NK cells within the CNS of EAE mice revealed that ChAT$^+$ NK cells were a small population (Fig. 2*F* and Fig. S3), the chemoattractive effect and intercellular communication seemed to "recruit" ChAT$^+$ NK cells to accumulate around the CCR2$^+$Ly6C^{hi} monocytes at inflammatory sites. The intercellular action is critical in shaping the immune activities of NK cells (19, 20, 22, 59), especially the activating effect of Ly6C^{hi} monocytes toward NK cells (30). Reciprocally, activated NK cells can influence the ability of proinflammatory monocytes to regulate immunity (21, 60, 61). In our experiments, ChAT$^+$ NK cells reciprocally interacted with CCR2$^+$Ly6C^{hi} monocytes through chemokine and cytokine secretion, thus regulating the immune functions of these cells.

NK cells are reported to engage in cross-talk with macrophages through various cytokines and are also contact-dependent within the immune synapse (60). The cytolytic effects toward target cells are based on the balance between the activated receptor NKG2D

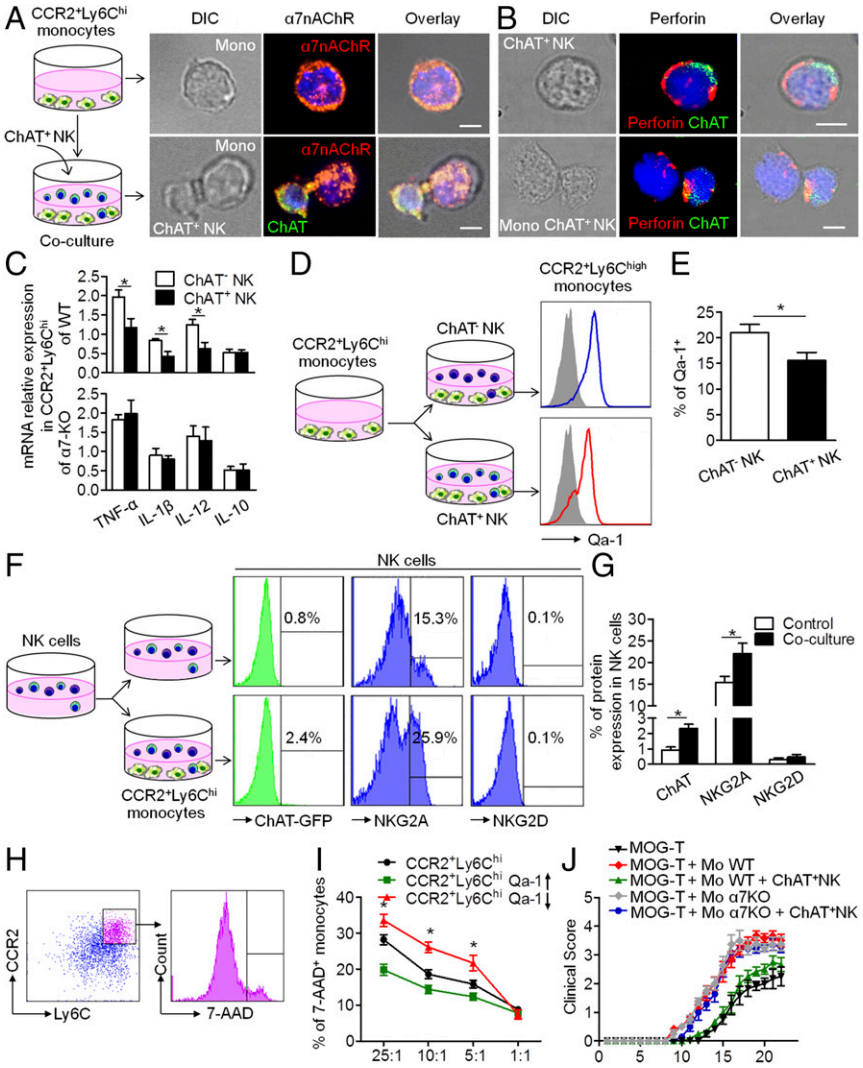

Fig. 7. Immune synapse between ChAT$^+$ NK cells and CCR2$^+$Ly6C^{hi} monocytes involved the NKG2A–Qa-1 pathway and α7nAChR. (*A*) CCR2$^+$Ly6C^{hi} monocytes were cocultured with ChAT$^+$ NK cells. α7nAChRs were evenly distributed on the surfaces of CCR2$^+$Ly6C^{hi} monocytes alone but accumulated at the immune synapse with ChAT$^+$ NK cells. Images represent three independent experiments. DIC, differential interference contrast. (Scale bars, 2 μm.) (*B*) Cytotoxic granules containing perforin were polarized in ChAT$^+$ NK cells toward CCR2$^+$Ly6C^{hi} monocytes but evenly distributed when NK cells were cultured alone. Images represent three independent experiments. (Scale bars, 2 μm.) (*C*) The expression of TNF-α, IL-1β, and IL-12 in CCR2$^+$Ly6C^{hi} monocytes from WT mice decreased after coculture with ChAT$^+$ NK cells, whereas this expression remained unchanged in α7nAChR KO CCR2$^+$Ly6C^{hi} monocytes in the coculture system. There was no difference in IL-10 expression. $n = 6$ per group from three independent experiments. (*D* and *E*) Qa-1 expression on CCR2$^+$Ly6C^{hi} monocytes was down-regulated after culture with ChAT$^+$ NK cells. (*F* and *G*) NK cells were cocultured with CCR2$^+$Ly6C^{hi} monocytes. Thereafter, the expression of ChAT-eGFP and NKG2A increased in NK cells; NKG2D remained consistent. $n = 6$ per group from three independent experiments for *D*–*G*. (*H* and *I*) The viability of CCR2$^+$Ly6C^{hi} monocytes in the coculture system was evaluated by 7-AAD staining. Qa-1 expression up-regulated by lentivirus transfection in CCR2$^+$Ly6C^{hi} monocytes rendered them less susceptible to killing by NK cells, whereas down-regulation exacerbated the killing. $n = 6$ per group from two independent experiments. (*J*) ChAT$^+$ NK cell implantation alleviated symptoms reflected in high clinical scores of EAE mice administered MOG-responsive T cells and CCR2$^+$Ly6C^{hi} monocytes of WT, but had no effect on EAE mice given α7nAChR KO CCR2$^+$Ly6C^{hi} monocytes. $n = 9$ per group from three independent experiments. Mean ± SEM. $^*P < 0.05$.

and the inhibitory receptor NKG2A (62–64). Results from our microassays indicated that the ChAT$^+$ NK cells had no increase of cytolytic activity, which was confirmed in vitro by a cytotoxic assay of YAC-1 cells (Fig. S4 *A* and *B*). However, the specific lysis of autologous CCR2$^+$Ly6C^{hi} monocytes in coculture with ChAT$^+$ NK cells was higher than that with the ChAT$^-$ subset (Fig. S4 *A* and *B*). Actually, this "cytotoxicity" toward autologous immune cells was largely due to the lack of Qa-1 on CCR2$^+$Ly6C^{hi} monocytes cultured with ChAT$^+$ NK cells, because Qa-1 reduction broke down the immune tolerance of those cells under the surveillance of autologous NK cells, instead of the cytotoxicity of the NK cells themselves (Fig. 7*D*). Besides, the ligands for NKG2D, RAE-1, and MULT-1 on CCR2$^+$Ly6C^{hi} monocytes were not altered significantly after culture with ChAT$^+$ NK cells (Fig. S4*C*), indicating how important the NKG2A–Qa-1 pathway may be as a mediator of this activity. The ligands expressed in CCR2$^+$Ly6C^{hi} monocytes of the CNS by ChAT$^+$ NK cell implantation also represented the down-regulation of Qa-1 in vivo (Fig. S4 *D* and *E*), although the reason for that down-regulation remains unclear and in need of inquiry. The redistribution of α7nAChRs accumulated in the immune synapse might constitute a basic structure for the cholinergic antiinflammatory effect of locally concentrated ACh derived from ChAT$^+$ NK cells. The down-regulation of Qa-1 in CCR2$^+$Ly6C^{hi} monocytes was observed upon nicotine treatment in culture or in adoptively transferred EAE with ChAT$^+$ NK cell implantation, activity that was reversed by α7nAChR KO (Fig. S4 *F* and *G*), thus suggesting involvement of the cholinergic effect as well as α7nAChRs in regulating Qa-1 expression.

The up-regulation of ChAT expression under abnormal autoimmune conditions was verified in peripheral NK cells from MS patients (Fig. S5 *A*–*C*). Further experiments confirmed that these changes resulted mainly from the up-regulation of ChAT expression in CD56^{bright} subsets of NK cells (Fig. S5 *D*–*F*), which were reported to be activated under MS conditions rather than the CD56^{dim}CD16^{bright} NK cells (15). Unlike murine NK cells, human NK subsets did not show a simple increase in ChAT expression along with their maturation from CD56^{bright} to CD16^{bright} NK cells in normal conditions; an up-regulation in CD56^{bright} subsets was found only in MS patients. Therefore, ACh synthesis seems to be largely affected by inflammatory circumstances, and the functional response occurs along with mobilization of this subset of NK cells. CD56^{bright} NK cells have been known to play important roles in MS, including a heightened capacity for migration from the periphery into the CNS and accumulation in the demyelinated lesions where they interact with local immune cells (15). Importantly, CD56^{bright} NK cells in the peripheral circulation were found to undergo MS-related activation, although the CD56^{dim}CD16^{bright} subpopulation decreased (15). This cholinergic up-regulation could be induced by

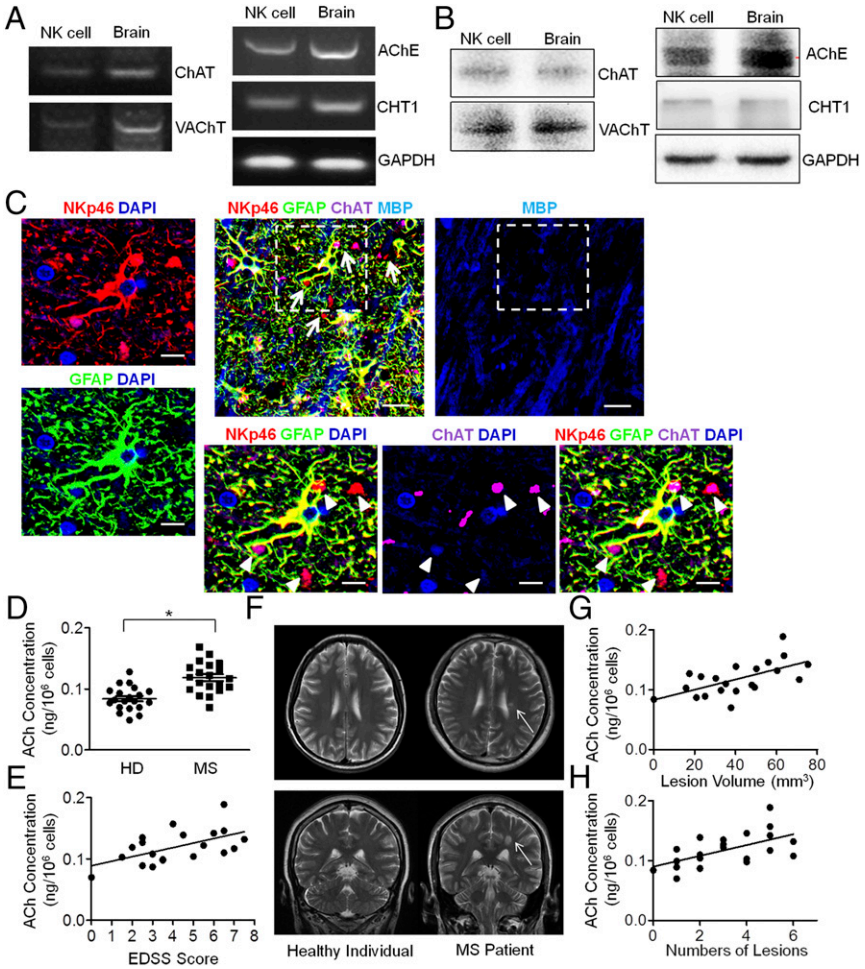

Fig. 8. Cholinergic system of human NK cells and the up-regulation of ACh synthesis in MS patients. (*A* and *B*) Components of the cholinergic system (ChAT, VAChT, AChE, CHT1) were identified in human NK cells by RT-PCR and Western blot, compared with the positive control from brain samples. PCR bands: ChAT, 403 bp; VAChT, 284 bp; AChE, 163 bp; CHT1, 385 bp; GAPDH, 120 bp; Western blot bands: ChAT, 68 kDa; VAChT, 72 kDa; AChE, 68 kDa; CHT1, 51 kDa; GAPDH, 36 kDa. $n = 5$. (*C*) Cells with NKp46 expression (*Upper Middle*) were found mostly in areas with demyelination of white matter, as reflected by the MBP staining (*Upper Right*). White matter lesions infiltrating NK cells were identified as $NKp46^{+}GFAP^{-}$, as the arrows indicate (*Upper Middle*). (Scale bars, 20 μm.) Images with higher magnification of the dashed box indicated area are shown to depict the NK cells ($NKp46^{+}GFAP^{-}$) (arrowheads) (*Lower Left*) with ChAT expression (*Lower Right*). (Scale bars, 8 μm.) Images are representative of six individuals. (*D*) UPLC-MS/MS detection of intracellular ACh production from human NK cells showed higher levels in MS patients compared with healthy individuals (HD). $n = 20$ per group. (*E*) The intracellular ACh concentrations from NK cells of MS patients also correlated with the EDSS scores. $n = 20$ per group. $P < 0.05$. (*F*) Images of axial and coronal T2 MRIs showed hyperintensity of the demyelinated lesions around the peripheral ventricles. Representative images from $n = 20$ per group. (*G* and *H*) MRI scanning showed a positive correlation between intracellular ACh concentration and lesion volume ($P < 0.05$) or numbers of lesions ($P < 0.05$). $n = 20$ per group. Mean ± SEM. $^{*}P < 0.05$.

the overactivated inflammatory environment, which in turn might exert immunosuppressive effects to counteract the internal immune responses. Potentially, determining intracellular ACh concentrations in such patients could provide a prognostic method for estimating the severity of disease and offer a new strategy for MS intervention.

Materials and Methods

Detailed information on materials and methods used in this study is provided in *SI Materials and Methods*.

Mice. C57BL/6 WT mice were purchased from Vital River. ChAT-eGFP, $CX3CR1^{GFP/GFP}$ ($CX3CR1^{-/-}$), and α7nAChR KO mice were purchased from the Jackson Laboratory. $Rag2^{-/-}$ $\gamma c^{-/-}$ mice were purchased from Taconic Biosciences. EAE and adoptively transferred EAE were induced in these animals as described. The experiments were reviewed and approved by the animal care and use committees of Tianjin Medical University and Tianjin Neurological Institute.

FACS Analysis and FACS Sorting. Isolated immune cells were assessed and sorted according to standard protocols.

PCR. cDNA was prepared from sorted cells or indicated tissues, and RT-PCR was performed with the outer primers (Table S1). For quantitative determination, qRT-PCR was performed with template and primers as displayed in Table S2.

UPLC-MS/MS. Isolated NK cells were homogenized and deproteinized. Supernatants with an internal standard (d_9-ACh; CDN) added were obtained for UPLC-MS/MS analysis. The conditions of the system were adjusted following the parameters as published (36).

Cellular Transplantation. A total volume of 10 μL NK cells suspended at a concentration of 5×10^6 per mL was loaded into a 10-μL Hamilton syringe. The amount of NK cells to be implanted into the CNS was determined by dose-dependent quantification (Fig. S6). EAE was induced in $CX3CR1^{-/-}$ mice, with cells or vehicles injected into their lateral cerebral ventricles at ~10 to 13 dpi.

Neuropathology and Neuroimaging. Samples were prepared for H&E (Solarbio), LFB, and immunofluorescent staining. MRI was performed using a 7-T small-animal MRI instrument for acquiring T2-weighted images.

Cell Culture and Migratory, Conjugative, and Viability Assays. After isolation, cells were cultured under the indicated conditions for migration, conjugation (65–67), lentivirus transfection, and viability assays as described.

Human Subjects and Quantification of NK Cell-Derived ACh. Brain sections from patients with relapsing–remitting MS were acquired from the Sun Health Research Institute and St. Joseph's Hospital and examined retrospectively. The protocols and informed consent were approved by the Institutional Review Board of the Banner Sun Health Institute and St. Joseph's Hospital. Patients or their caregivers provided informed consent for brain donation as well as for the purpose of research analysis. Thirty-eight patients with relapsing–remitting MS at the acute stage of the disease were enrolled in this study (Table S3). The protocol was approved by Tianjin Medical University General Hospital, and informed consent was obtained from all patients at enrollment.

ACKNOWLEDGMENTS. We acknowledge Dr. R. Xiang (Nankai University), Dr. Y. Liu (Capital Medical University), Dr. W. Yang (Chinese Academy of Medical Sciences and Peking Union Medical College), and Mr. Y. Xia (Tianjin Centers for Disease Control and Prevention) for kindly sharing laboratory equipment as well as technical expertise. This study was supported in part by the National Natural Science Foundation of China Grants 81571600, 81322018, 81273287, 81100887, and 81471535; and the Youth Top-Notch Talent Support Program.

1. Compston A, Coles A (2002) Multiple sclerosis. *Lancet* 359:1221–1231.
2. Ransohoff RM (2012) Animal models of multiple sclerosis: The good, the bad and the bottom line. *Nat Neurosci* 15:1074–1077.
3. Borovikova LV, et al. (2000) Vagus nerve stimulation attenuates the systemic inflammatory response to endotoxin. *Nature* 405:458–462.
4. Kawashima K, Fujii T (2003) The lymphocytic cholinergic system and its contribution to the regulation of immune activity. *Life Sci* 74:675–696.
5. Rosas-Ballina M, et al. (2011) Acetylcholine-synthesizing T cells relay neural signals in a vagus nerve circuit. *Science* 334:98–101.
6. Reardon C, et al. (2013) Lymphocyte-derived ACh regulates local innate but not adaptive immunity. *Proc Natl Acad Sci USA* 110:1410–1415.
7. Liu Q, et al. (2016) Neural stem cells sustain natural killer cells that dictate recovery from brain inflammation. *Nat Neurosci* 19:243–252.
8. Shi FD, Ljunggren HG, La Cava A, Van Kaer L (2011) Organ-specific features of natural killer cells. *Nat Rev Immunol* 11:658–671.
9. Morandi B, et al. (2008) Role of natural killer cells in the pathogenesis and progression of multiple sclerosis. *Pharmacol Res* 57:1–5.
10. Chanvillard C, Jacolik RF, Infante-Duarte C, Nayak RC (2013) The role of natural killer cells in multiple sclerosis and their therapeutic implications. *Front Immunol* 4:63.
11. Bielekova B, et al. (2006) Regulatory CD56(bright) natural killer cells mediate immunomodulatory effects of IL-2Ralpha-targeted therapy (daclizumab) in multiple sclerosis. *Proc Natl Acad Sci USA* 103:5941–5946.
12. Sheridan JP, Robinson RR, Rose JW (2014) Daclizumab, an IL-2 modulating antibody for treatment of multiple sclerosis. *Expert Rev Clin Pharmacol* 7:9–19.
13. Giovannoni G, et al.; SELECTION Study Investigators (2014) Daclizumab high-yield process in relapsing-remitting multiple sclerosis (SELECTION): A multicentre, randomised, double-blind extension trial. *Lancet Neurol* 13:472–481.
14. Kappos L, et al. (2015) Daclizumab HYP versus interferon beta-1a in relapsing multiple sclerosis. *N Engl J Med* 373:1418–1428.
15. Gross CC, et al. (2016) Impaired NK-mediated regulation of T-cell activity in multiple sclerosis is reconstituted by IL-2 receptor modulation. *Proc Natl Acad Sci USA* 113: E2973–E2982.
16. Wiendl H, Gross CC (2013) Modulation of IL-2Rα with daclizumab for treatment of multiple sclerosis. *Nat Rev Neurol* 9:394–404.
17. Hao J, et al. (2011) Interleukin-2/interleukin-2 antibody therapy induces target organ natural killer cells that inhibit central nervous system inflammation. *Ann Neurol* 69: 721–734.
18. Hao J, et al. (2010) Central nervous system (CNS)-resident natural killer cells suppress Th17 responses and CNS autoimmune pathology. *J Exp Med* 207:1907–1921.
19. Baratin M, et al. (2005) Natural killer cell and macrophage cooperation in MyD88-dependent innate responses to *Plasmodium falciparum*. *Proc Natl Acad Sci USA* 102: 14747–14752.
20. Nedvetzki S, et al. (2007) Reciprocal regulation of human natural killer cells and macrophages associated with distinct immune synapses. *Blood* 109:3776–3785.
21. Bellora F, et al. (2010) The interaction of human natural killer cells with either unpolarized or polarized macrophages results in different functional outcomes. *Proc Natl Acad Sci USA* 107:21659–21664.
22. Soderquest K, et al. (2011) Monocytes control natural killer cell differentiation to effector phenotypes. *Blood* 117:4511–4518.
23. Simard AR, Soulet D, Gowing G, Julien JP, Rivest S (2006) Bone marrow-derived microglia play a critical role in restricting senile plaque formation in Alzheimer's disease. *Neuron* 49:489–502.
24. Mildner A, et al. (2009) $CCR2^{+}$Ly-$6C^{hi}$ monocytes are crucial for the effector phase of autoimmunity in the central nervous system. *Brain* 132:2487–2500.
25. Gautier EL, et al.; Immunological Genome Consortium (2012) Gene-expression profiles and transcriptional regulatory pathways that underlie the identity and diversity of mouse tissue macrophages. *Nat Immunol* 13:1118–1128.
26. Yamasaki R, et al. (2014) Differential roles of microglia and monocytes in the inflamed central nervous system. *J Exp Med* 211:1533–1549.
27. Ajami B, Bennett JL, Krieger C, McNagny KM, Rossi FM (2011) Infiltrating monocytes trigger EAE progression, but do not contribute to the resident microglia pool. *Nat Neurosci* 14:1142–1149.
28. Moreno M, et al. (2014) Conditional ablation of astroglial CCL2 suppresses CNS accumulation of M1 macrophages and preserves axons in mice with MOG peptide EAE. *J Neurosci* 34:8175–8185.
29. Croxford AL, et al. (2015) The cytokine GM-CSF drives the inflammatory signature of $CCR2^{+}$ monocytes and licenses autoimmunity. *Immunity* 43:502–514.
30. Coombes JL, Han SJ, van Rooijen N, Raulet DH, Robey EA (2012) Infection-induced regulation of natural killer cells by macrophages and collagen at the lymph node subcapsular sinus. *Cell Reports* 2:124–135.
31. Shi FD, et al. (2009) Nicotinic attenuation of central nervous system inflammation and autoimmunity. *J Immunol* 182:1730–1739.
32. Hao J, et al. (2011) Attenuation of CNS inflammatory responses by nicotine involves α7 and non-α7 nicotinic receptors. *Exp Neurol* 227:110–119.
33. Simard AR, et al. (2013) Differential modulation of EAE by α9*- and β2*-nicotinic acetylcholine receptors. *Immunol Cell Biol* 91:195–200.
34. Jiang W, et al. (2016) Infiltration of $CCR2^{+}Ly6C^{high}$ proinflammatory monocytes and neutrophils into the central nervous system is modulated by nicotinic acetylcholine receptors in a model of multiple sclerosis. *J Immunol* 196:2095–2108.
35. St-Pierre S, et al. (2016) Nicotinic acetylcholine receptors modulate bone marrow-derived pro-inflammatory monocyte production and survival. *PLoS One* 11:e0150230.
36. Zhang C, et al. (2016) Determination of non-neuronal acetylcholine in human peripheral blood mononuclear cells by use of hydrophilic interaction ultra-performance liquid chromatography-tandem mass spectrometry. *J Chromatogr B Analyt Technol Biomed Life Sci* 1022:265–273.
37. Hayakawa Y, Smyth MJ (2006) CD27 dissects mature NK cells into two subsets with distinct responsiveness and migratory capacity. *J Immunol* 176:1517–1524.
38. Chiossone L, et al. (2009) Maturation of mouse NK cells is a 4-stage developmental program. *Blood* 113:5488–5496.
39. Huang D, et al. (2006) The neuronal chemokine CX3CL1/fractalkine selectively recruits NK cells that modify experimental autoimmune encephalomyelitis within the central nervous system. *FASEB J* 20:896–905.
40. Gan Y, et al. (2014) Ischemic neurons recruit natural killer cells that accelerate brain infarction. *Proc Natl Acad Sci USA* 111:2704–2709.
41. Winger RC, et al. (2016) Cutting edge: CD99 is a novel therapeutic target for control of T cell-mediated central nervous system autoimmune disease. *J Immunol* 196: 1443–1448.
42. Durrenberger PF, et al. (2012) Innate immunity in multiple sclerosis white matter lesions: Expression of natural cytotoxicity triggering receptor 1 (NCR1). *J Neuroinflammation* 9:1.
43. Wang H, et al. (2003) Nicotinic acetylcholine receptor alpha7 subunit is an essential regulator of inflammation. *Nature* 421:384–388.
44. Tracey KJ (2009) Reflex control of immunity. *Nat Rev Immunol* 9:418–428.
45. Andersson U, Tracey KJ (2012) Neural reflexes in inflammation and immunity. *J Exp Med* 209:1057–1068.
46. Huntington ND, Vosshenrich CA, Di Santo JP (2007) Developmental pathways that generate natural-killer-cell diversity in mice and humans. *Nat Rev Immunol* 7: 703–714.
47. Kaur G, Trowsdale J, Fugger L (2013) Natural killer cells and their receptors in multiple sclerosis. *Brain* 136:2657–2676.
48. Poli A, et al. (2013) NK cells in central nervous system disorders. *J Immunol* 190: 5355–5362.
49. Peng H, Tian Z (2014) NK cell trafficking in health and autoimmunity: A comprehensive review. *Clin Rev Allergy Immunol* 47:119–127.
50. Walzer T, Vivier E (2011) G-protein-coupled receptors in control of natural killer cell migration. *Trends Immunol* 32:486–492.
51. Fletcher JM, Lalor SJ, Sweeney CM, Tubridy N, Mills KH (2010) T cells in multiple sclerosis and experimental autoimmune encephalomyelitis. *Clin Exp Immunol* 162:1–11.
52. Wolf SD, Dittel BN, Hardardottir F, Janeway CA, Jr (1996) Experimental autoimmune encephalomyelitis induction in genetically B cell-deficient mice. *J Exp Med* 184: 2271–2278.
53. Shi FD, Van Kaer L (2006) Reciprocal regulation between natural killer cells and autoreactive T cells. *Nat Rev Immunol* 6:751–760.
54. Waisman A, Liblau RS, Becher B (2015) Innate and adaptive immune responses in the CNS. *Lancet Neurol* 14:945–955.
55. Hammond MD, et al. (2014) $CCR2^{+}$ $Ly6C^{(hi)}$ inflammatory monocyte recruitment exacerbates acute disability following intracerebral hemorrhage. *J Neurosci* 34:3901–3909.
56. Mishra MK, Wang J, Silva C, Mack M, Yong VW (2012) Kinetics of proinflammatory monocytes in a model of multiple sclerosis and its perturbation by laquinimod. *Am J Pathol* 181:642–651.
57. Palframan RT, et al. (2001) Inflammatory chemokine transport and presentation in HEV: A remote control mechanism for monocyte recruitment to lymph nodes in inflamed tissues. *J Exp Med* 194:1361–1373.
58. Si Y, Tsou CL, Croft K, Charo IF (2010) CCR2 mediates hematopoietic stem and progenitor cell trafficking to sites of inflammation in mice. *J Clin Invest* 120:1192–1203.
59. Rölle A, et al. (2014) IL-12-producing monocytes and HLA-E control HCMV-driven $NKG2C^{+}$ NK cell expansion. *J Clin Invest* 124:5305–5316.
60. Michel T, Hentges F, Zimmer J (2013) Consequences of the crosstalk between monocytes/macrophages and natural killer cells. *Front Immunol* 3:403.
61. Tosello-Trampont AC, et al. (2016) NKp46(+) natural killer cells attenuate metabolism-induced hepatic fibrosis by regulating macrophage activation in mice. *Hepatology* 63: 799–812.
62. Kruse PH, Matta J, Ugolini S, Vivier E (2014) Natural cytotoxicity receptors and their ligands. *Immunol Cell Biol* 92:221–229.
63. Koch J, Steinle A, Watzl C, Mandelboim O (2013) Activating natural cytotoxicity receptors of natural killer cells in cancer and infection. *Trends Immunol* 34:182–191.
64. Fang M, et al. (2011) CD94 is essential for NK cell-mediated resistance to a lethal viral disease. *Immunity* 34:579–589.
65. Barber DF, Long EO (2003) Coexpression of CD58 or CD48 with intercellular adhesion molecule 1 on target cells enhances adhesion of resting NK cells. *J Immunol* 170: 294–299.
66. Burshtyn DN, Davidson C (2010) Natural killer cell conjugate assay using two-color flow cytometry. *Methods Mol Biol* 612:89–96.
67. Burshtyn DN, Shin J, Stebbins C, Long EO (2000) Adhesion to target cells is disrupted by the killer cell inhibitory receptor. *Curr Biol* 10:777–780.